

Modeling DMPC lipid membranes with SIRAH force-field

Exequiel E. Barrera¹ · Ezequiel N. Frigini² · Rodolfo D. Porasso² · Sergio Pantano¹

Received: 31 March 2017 / Accepted: 19 July 2017
© Springer-Verlag GmbH Germany 2017

Abstract Coarse-grained simulation schemes are increasingly gaining popularity in the scientific community because of the significant speed up granted, allowing a considerable expansion of the accessible time and size scales accessible to molecular simulations. However, the number of compatible force fields capable of representing ensembles containing different molecular species (i.e., Protein, DNA, etc) is still limited. Here, we present a set of parameters and simplified representation for lipids compatible with the SIRAH force field for coarse-grained simulations (<http://www.sirahff.com>). We show that the present model not only achieves a correct reproduction of structural parameters as area per lipid and thickness, but also dynamic descriptors such as diffusion coefficient, order parameters, and proper temperature driven variations. Adding phospholipid membranes to the existing aqueous solution, protein and DNA representations of the SIRAH force field permit considering the most common problems tackled by the biomolecular simulation community.

Keywords Coarse-grained models · DMPC · Lipid membranes · Molecular dynamics

This paper belongs to Topical Collection QUITEL 2016

✉ Exequiel E. Barrera
ebarrera@pasteur.edu.uy

¹ Biomolecular Simulations Group, Institut Pasteur de Montevideo, Mataojo 2020, 11400 Montevideo, Uruguay

² Instituto de Matemática Aplicada San Luis (IMASL), CONICET, Facultad de Ciencias Físico Matemáticas y Naturales, Universidad Nacional de San Luis, Av. Ejército de los Andes 950, 5700 San Luis, Argentina

Introduction

The application of GPU acceleration on molecular dynamics (MD) simulations combined with coarse grained (CG) models allows the study of biological systems beyond the order of 10^6 particles with modest computational resources, thus encouraging us to rethink the design and size of our simulation boxes [1]. In this sense, there is great interest in the generation of parameters for lipid molecules that could act as building blocks to model different arrangements of membranes such as planar bilayers, micelles, vesicles, etc. In particular, phospholipids are the main lipid constituent of eukaryotic cell membranes and its inclusion in *in silico* experiments opens the possibility to study different biological scenarios where the compartmentalization and scaffold provided by lipid bilayers is fundamental. The study of cell penetrating peptides [2, 3], transmembrane protein behavior [4, 5], cell membrane potentials [6], and vesicular transport [7, 8] are just some of the many possibilities of systems to explore in the continuous expanding field of biomolecular simulations.

Our group has developed a CG force field for biomolecules named SIRAH (<http://www.sirahff.com>) using a standard pairwise Hamiltonian common to most MD simulation packages containing topologies and parameters for DNA [9] and proteins [10]. Here, we present the parameterization of the phospholipid 1,2-dimyristoyl-sn-glycero-3-phosphocholine (DMPC), adding a new type of biological molecule to the SIRAH force field. Even though CG models for lipids have been profusely developed by different groups [11–14], their inclusion in our force field combined with the explicit CG representation of aqueous solvation named WatFour and CG electrolytes [15], generates a broad set of parameters to simulate biomolecular systems that overcome some common limitations of other CG force fields like the use of uniform dielectric constant, implicit or no ionic strength effect, lack of

long-range interactions, use of topological information to maintain the secondary structure, etc.

Methods

Derivation of the model

In accord with the SIRAH's philosophy, the parameterization of the phospholipid was pursued following a top-down approach fitting structural features, such as area per lipid (AL), thickness, and density profiles of different species across the computational box. The election of DMPC was due to its simplicity and other phospholipids containing unsaturated acyl chains and different polar heads will be presented in a future publication. The CG representation for DMPC was modeled following the mapping scheme proposed by Shelley et al. [16]. To ensure the compatibility with previous protein parameters we used bead types representing functional groups already present in the SIRAH force field [10]. The non-bonded interaction parameters are indicated for each bead in Fig. 1. All intermolecular interactions are calculated within the same Hamiltonian function used by standard MD simulations (see Computational details).

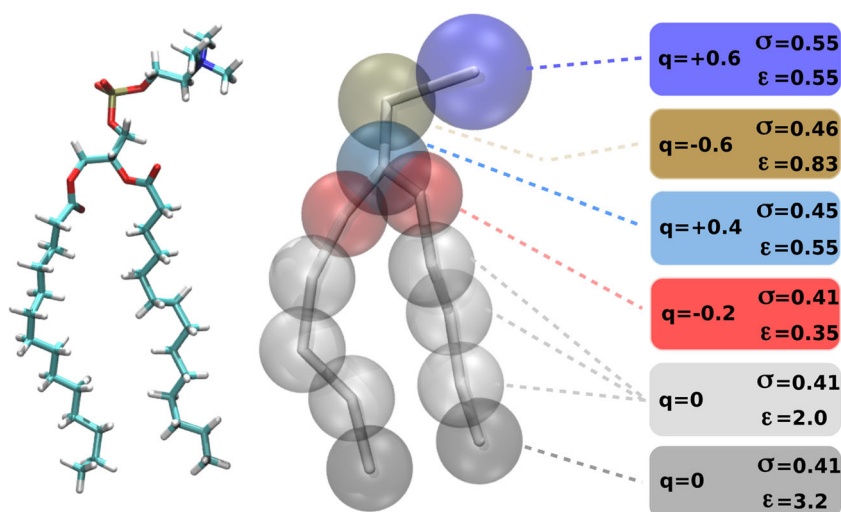
Van der Waals (vdW) interactions between choline and phosphate beads are not calculated according to the Lorentz-Berthelot combination rules. We set these specific corrections to avoid over stabilization of salt bridges between these polar beads [10]. The partial charge distribution was assigned with the simple criterion of charge groups that add up to zero or a integer number for each molecule [10]. Beads were represented with a uniform mass of 50 a.u., bonded with spring constants of $41,840 \text{ kJ mol}^{-1} \text{ nm}^{-2}$, and angle bending constants of $627.6 \text{ kJ mol}^{-1} \text{ rad}^{-2}$ for polar heads, i.e., the same parameters used for CG models of protein and DNA. We test varying

angle bending constants for lipid tails within a range of $10 \text{ kJ mol}^{-1} \text{ rad}^{-2}$ to $20 \text{ kJ mol}^{-1} \text{ rad}^{-2}$, evaluating AL and thickness values. We finally choose a value of $14 \text{ kJ mol}^{-1} \text{ rad}^{-2}$, which fits better with experimental data. Equilibrium distances for bond and angular stretching were taken from Shelley et al. [16].

Computational details

Starting configurations were generated with PACKMOL [17], obtaining patches composed of 64 and 128 DMPC molecules per leaflet, the larger DMPC bilayer was employed for its study in ionic solutions. The fine grain bilayers were converted to CG using an ad hoc script included in SIRAH Tools [18]. Simulations were performed using GROMACS 2016.1 (<http://www.gromacs.org>) [1] with a time step of 20 fs updating the neighbor list every 10 steps. Electrostatic interactions were calculated using particle mesh Ewald (PME) [19] with a direct cut off of 1.2 nm using the same value for interactions. Energy minimization involved 5000 iterations using the steepest descent algorithm. All systems were equilibrated for 5 ns applying positional restraints of $1000 \text{ kJ mol}^{-1} \text{ nm}^{-2}$ to all heavy atoms of DMPC, employing an isothermal-isobaric (NPT) ensemble. Production MD simulations were carried out for 1 μs in the absence of any restraints at four different temperatures (303 K, 313 K, 323 K, and 333 K) using the v-rescale thermostat [20] and keeping pressure at 1 bar by means of the Parrinello-Rahman barostat [21] under semi-isotropic conditions. Three independent trajectories were produced for each system by generating different initial random velocities. The analysis of the simulations was performed over the last 500 ns of the simulation using the analysis tools provided in the Gromacs package. The AL was obtained dividing the average area of the simulation box in the X-Y directions by the number of DMPC molecules corresponding to one leaflet

Fig. 1 Atomistic and CG representations of DMPC. Charges are indicated in electron units while vdW parameters are in nm and kJ mol^{-1} for sigma and epsilon, respectively



of the bilayer. The bilayer thickness was calculated measuring the average distance considering only the z-axis between the centers of mass of the phosphorous beads in each leaflet, minimizing the errors due to lateral fluctuations. The lateral diffusion was computed using the Einstein relation based on the average lateral mean squared displacement (MSD) and calculated over the position of the phosphate beads. Acyl order parameters were calculated with the program gmx order.

Results and discussion

Once we simulated for 1 μ s in a NPT ensemble the CG DMPC bilayers, we focused our analysis on common properties that have been extensively used as force-field validation strategies [22]. These include structural (namely density profiles along the z-axis, interfacial AL, and bilayer thickness) and dynamic properties such as lipid lateral diffusion coefficient. We also assessed the ability of the force field to reproduce the effects that temperature exerts over the properties mentioned above and compared them with experimental values previously reported by Kučerka et al. [23].

Density profiles

The overall shape of the electron density profile for DMPC was correctly reproduced with our CG parameters. Figure 2 depicts the position of peaks for DMPC, phosphate beads, CG water (called WatFour or WT4 for shortness), and CG counterions. A proper hydrophobic-hydrophilic distribution could be observed, with water molecules not penetrating beyond the phosphate groups peaks. In the case of CG cations both K^+ and Na^+ showed a partial approach to the phosphate beads driven by electrostatic attraction, having higher densities on the bulk solvent region of the box. This behavior could be explained considering that CG SIRAH ions possess vdW radii that match the first minima of the radial distribution function of hydrated ions as obtained from the neutron diffraction experiment [24], roughly considering an implicit first solvation shell. On the other hand, bigger Cl^- ions were mainly distributed in the bulk away from the polar heads.

Area per lipid

The interfacial AL constitutes an essential property of lipid bilayers being directly related with its level of fluidity. This property was analyzed over the last 500 ns of the three independent runs at 303 K and its averaged values were of 0.601 ± 0.007 nm² in close proximity with those published by Kučerka et al. (0.599 ± 0.012 nm²). As expected, systems simulated at higher temperatures resulted in increased values of AL as a consequence of the higher probability of trans-gauche isomerization [25]. In our simulation this

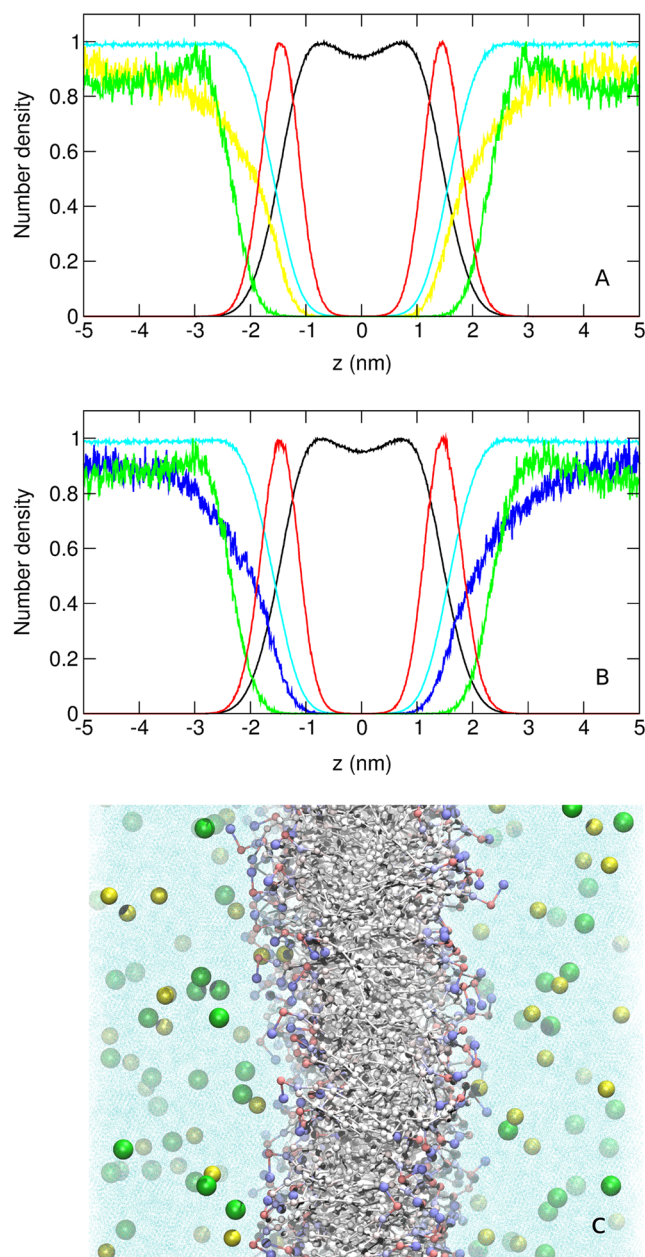


Fig. 2 Normalized number density profiles for DMPC solvated in 150 mM NaCl (a) and 150 mM KCl (b) electrolyte solutions. The profiles are divided in: whole DMPC (black), phosphate (red), WT4 (cyan), Na^+ (yellow), K^+ (blue), and Cl^- (green). Representative snapshot from the system solvated in NaCl (c)

isomerization is reproduced by the shift of the angles between the acyl chains beads toward lower values. This can be observed in the angular distribution plot represented in Fig. 3.

At 323 K AL values were in the range of the experimental uncertainty reported by Kučerka, while at 333 K this difference was approximately 5% higher (Fig. 4). This discrepancy is acceptable if we consider that published estimates of AL can vary significantly depending on the experimental observable on which the estimate is based and the model employed to interpret this data. Indeed, a recent review [22] that compiles

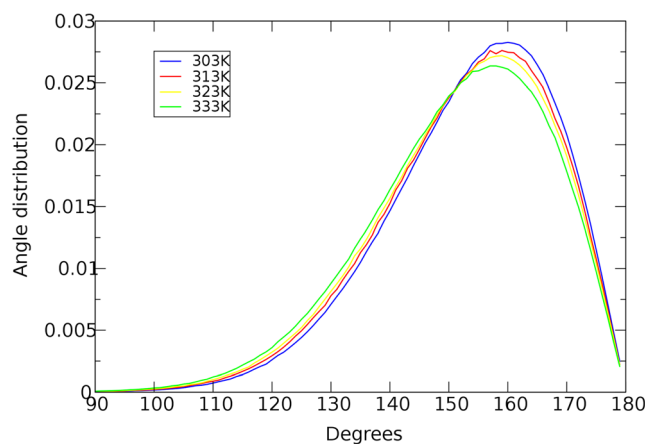


Fig. 3 Angular distribution for acyl chain beads for systems simulated at temperatures of 303 K (blue), 313 K (red), 323 K (yellow), and 333 K (green)

AL experimental values reveals variations ranging from 0.589 nm^2 to 0.652 nm^2 for DMPC at 300 K.

Thickness

There is a general agreement about how physical properties of membranes, specially its thickness, determines function, orientation, and sub-cellular localization of integral membrane proteins [26]. As seen in Fig. 5, thickness values obtained measuring the distance between the peaks of density profiles for phosphate beads were between 5% and 10% smaller than those published by Kučerka et al. Still, it is worth mentioning that these experimental results correspond to the overall bilayer thickness (D_B).

On the other hand, neutron scattering experiments estimate thickness with slightly higher values than those obtained by X-ray scattering [27]. This value is called head-head thickness (D_{HH}) and it is defined by the distance between the peaks of the phosphate head groups in the electron density profiles, giving more comparable results with those obtained by MD

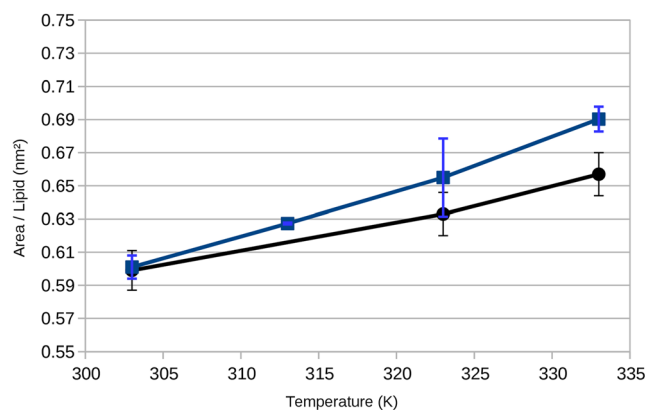


Fig. 4 Comparison between SIRAH MD simulations (blue squares) and experimental (black circles) area per lipid values as a function of temperature

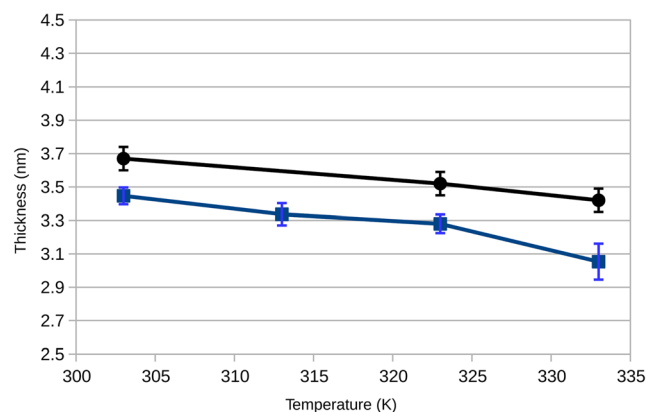


Fig. 5 Comparison between SIRAH MD simulations (blue squares) and experimental (black circles) thickness values as a function of temperature

simulations. Regarding the effect of temperature, once again the force field reproduced the correct experimental trend diminishing thickness from 303 K to 333 K.

Lateral diffusion coefficient

The time scales needed to measure translational self-diffusion are compatible with those reached by MD simulations (a few hundreds of nanoseconds) and for this reason is widely used to validate lipid force fields [22]. In order to avoid the overestimation of lateral diffusion created when studying small sized bilayers [28] the motion of the center of mass of the relevant leaflet was subtracted from the MSD of each lipid [29]. Lateral diffusion coefficient for motion parallel with the membrane plane (D_L) for DMPC at 303 K was $28.83 \mu\text{m}^2 \text{ s}^{-1}$. This resulted in good agreement with experimental measurements obtained by fluorescence recovery after photobleaching (FRAP) [30] applying a conversion factor of 4 (Table 1). Similar scaling has been previously reported for other CG force-field [11].

Acyl order parameters

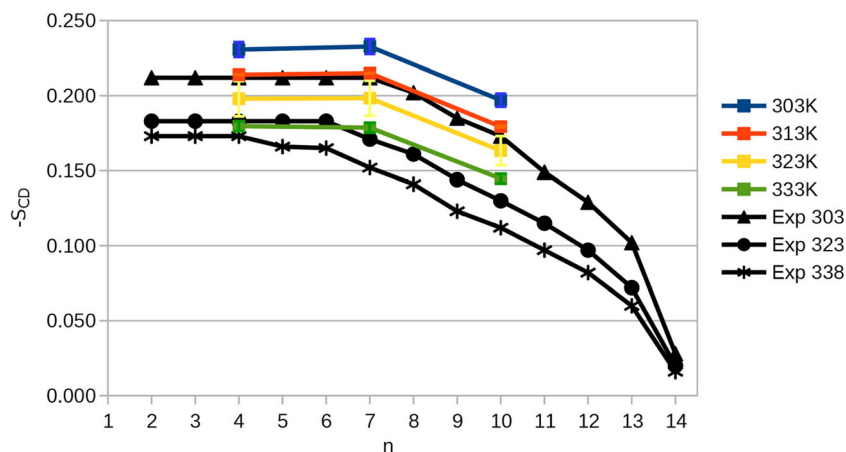
Lipid acyl chain order parameters are obtained by NMR spectroscopy using ^2H labeled lipids. In particular, the carbon-deuterium bond order parameter (S_{CD}) can be calculated from experimentally determined quadrupolar splittings [31] and

Table 1 Lateral diffusion coefficients for DMPC

	SIRAH force-field*	Experimental*
303 K	28.83 ± 2.739	6.9
313 K	46.55 ± 3.465	
323 K	64.07 ± 4.606	
333 K	84.27 ± 4.648	

* D_L values are expressed in $\mu\text{m}^2 \text{ s}^{-1}$

Fig. 6 Comparison of the order parameter $-S_{CD}$ obtained from ^2H NMR and MD simulations for sn_{-1} chains at different temperatures



compared directly with the values computed from MD simulations by means of Eq. (1).

$$S_z = \frac{3}{2} \cos^2 \theta_z - \frac{1}{2} \quad (1)$$

Since hydrogen is not represented in CG models we employed a well-known approximation measuring the angle θ_z between the z-axis of the simulation box and the vector from beads C_{n-1} to C_{n+1} [32]. Figure 6 shows the results averaged over the last 500 ns of simulation indicating that acyl order parameters present high similarity with experimental values informed by Petrache et al. [33]. In our case, considering the mapping conversion scheme of 1 CG bead every $3 C\alpha$, three values were obtained for each chain (sn_{-1} and sn_{-2}). For better visualization $-S_{CD}$ values are plotted only for chain sn_{-1} . The CG model for DMPC also showed lower order parameters when temperature increased from 303 K to 333 K in a similar fashion to the ^2H NMR experiments.

Conclusions

New CG parameters for DMPC have been tested and validated using different structural properties compared against experimental data, showing good concordance regarding area per lipid and thickness values, along with sensibility in temperature shifts. The distribution of different hydrophobic and polar groups and its relation with ionic species and water were also controlled reproducing correct density profiles. Not only structural but also dynamics features of the system were tested measuring lateral diffusion coefficients and acyl order parameters, the high resemblance of the results with those shown in literature let us conclude that the parameterization for DMPC is correct. Together with the previously reported CG models for DNA and proteins, the inclusion of the phospholipid DMPC extends the set of topologies offered by the SIRAH

force field for unbiased MD simulations with a speed up between 2 and 3 orders of magnitude, using explicit solvation and long-range electrostatics.

Acknowledgments This work was partially funded by FOCEM (MERCOSUR Structural Convergence Fund), COF 03/11. S.P. is researcher of the National Scientific Program of ANII (SNI). E.E.B. is beneficiary of a postdoctoral fellowship of CONICET. E.N.F. is beneficiary of a doctoral fellowship of CONICET (Consejo Nacional de Investigaciones Científicas y Técnicas, Argentina).

Compliance with ethical standards

Conflict of interest The authors declare that they have no conflict of interest.

References

- Abraham MJ et al. (2015) Gromacs: high performance molecular simulations through multi-level parallelism from laptops to supercomputers. *SoftwareX* 1:19–25. doi:10.1016/j.softx.2015.06.001
- Astrada S, Gomez Y, Barrera E, et al. (2016) Comparative analysis reveals amino acids critical for the anticancer activity of the peptide CIGB-552. *J Pept Sci* 22:711–722. doi:10.1002/psc.2934
- He X, Lin M, Sha B, et al. (2015) Coarse-grained molecular dynamics studies of the translocation mechanism of polyarginines across asymmetric membrane under tension. *Sci Rep* 5:12808. doi:10.1038/srep12808
- Herrera FE, Pantano S (2012) Structure and dynamics of nano-sized raft-like domains on the plasma membrane. *J Chem Phys* doi:10.1063/1.3672704
- Li Z-L, Ding H-M, Ma Y-Q (2016) Interaction of peptides with cell membranes: insights from molecular modeling. *J Phys Condens Matter* 28:83001–83018. doi:10.1088/0953-8984/28/8/083001
- Herrera FE, Pantano S (2009) Salt induced asymmetry in membrane simulations by partial restriction of ionic motion. *J Chem Phys* 130:1–9. doi:10.1063/1.3132705
- Knecht V, Marrink S-J (2007) Molecular dynamics simulations of lipid vesicle fusion in atomic detail. *Biophys J* 92:4254–4261. doi:10.1529/biophysj.106.103572
- Tamai H, Okutsu N, Tokuyama Y, et al. (2016) A coarse grained molecular dynamics study on the structure and stability of small-

- sized liposomes. *Mol Simul* 42:122–130. doi:10.1080/08927022.2015.1020487
9. Dans PD, Zeida A, Machado MR, Pantano S (2010) A coarse grained model for atomic-detailed DNA simulations with explicit electrostatics. *J Chem Theory Comput* 6:1711–1725. doi:10.1021/ct900653p
 10. Darré L, Machado MR, Brandner AF, et al. (2015) SIRAH: a structurally unbiased coarse-grained force field for proteins with aqueous solvation and long-range electrostatics. *J Chem Theory Comput* 11:723–739. doi:10.1021/ct5007746
 11. Marrink S, Vries AD, Mark A (2004) Coarse grained model for semiquantitative lipid simulations. *J Phys Chem B* 108:750–760. doi:10.1021/jp036508g
 12. Shinoda W, DeVane R, Klein ML (2010) Zwitterionic lipid assemblies: molecular dynamics studies of monolayers, bilayers, and vesicles using a new coarse grain force field. *J Phys Chem B* 114:6836–6849. doi:10.1021/jp9107206.111
 13. Orsi M, Essex JW (2011) The ELBA force field for coarse-grain modeling of lipid membranes. *PLoS One* 6:e28637. doi:10.1371/journal.pone.0028637
 14. Lyubartsev AP (2005) Multiscale modeling of lipids and lipid bilayers. *Eur Biophys J* 35:53–61. doi:10.1007/s00249-005-0005-y
 15. Darre L, Machado MR, Dans PD, et al. (2010) Another coarse grain model for aqueous solvation: WAT FOUR? *J Chem Theory Comput* 6:3793–3797
 16. Shelley JC, Shelley MY, Reeder RC, et al. (2001) A coarse grain model for Phospholipid simulations a coarse grain model for phospholipid simulations. *J Phys Chem B* 105:4464–4470. doi:10.1021/jp010238p
 17. Martínez L, Andrade R, Birgin E, Martínez J (2010) Packmol: a package for building initial configurations for molecular dynamics simulations. *J Comput Chem* 30:2157–2164. doi:10.1002/jcc.21224
 18. Machado M, Pantano S (2016) Structural bioinformatics SIRAH Tools : mapping , backmapping and visualization of coarse-grained models. *Bioinformatics* 32:2–3. doi:10.1093/bioinformatics/btw020
 19. Darden TA, York D, Pedersen L (1993) Particle mesh Ewald: an N·log(N) method for Ewald sums in large systems. *J Chem Phys* 98:10089–10092. doi:10.1063/1.464397
 20. Bussi G, Donadio D, Parrinello M (2007) Canonical sampling through velocity rescaling. *J Chem Phys* 126:014101. doi:10.1063/1.2408420
 21. Parrinello M, Rahman A (1981) Polymorphic transitions in single crystals: a new molecular dynamics method. *J Appl Phys* 52:7182–7190. doi:10.1063/1.328693
 22. Poger D, Caron B, Mark AE (2015) Validating lipid force fields against experimental data: progress, challenges and perspectives. *Biochim Biophys Acta Biomembr* doi:10.1016/j.bbamem.2016.01.029
 23. Kučerka N, Nieh MP, Katsaras J (2011) Fluid phase lipid areas and bilayer thicknesses of commonly used phosphatidylcholines as a function of temperature. *Biochim Biophys Acta Biomembr* 1808:2761–2771. doi:10.1016/j.bbamem.2011.07.022
 24. Mancinelli R, Botti A, Bruni F, Ricci MA, Soper AK (2007) Perturbation of water structure due to monovalent ions in solution. *Phys Chem Chem Phys* 9:2959–2967. doi:10.1039/B701855J
 25. Cevc G, Marsh D (1987) *Phospholipid Bilayers: physical principles and models*. Wiley, New York
 26. Lee AG (2004) How lipids affect the activities of integral membrane proteins. *Biochim Biophys Acta Biomembr* 1666:62–87. doi:10.1016/j.bbamem.2004.05.012
 27. Kučerka N, Tristram-Nagle S, Nagle JF (2006) Structure of fully hydrated fluid phase lipid bilayers with monounsaturated chains. *J Membr Biol* 208:193–202. doi:10.1007/s00232-005-7006-8
 28. Roark M, Feller SE (2009) Molecular dynamics simulation study of correlated motions in phospholipid bilayer membranes. *J Phys Chem B* 113:13229–132234. doi:10.1021/jp902186f
 29. Lindahl E, Edholm O (2000) Mesoscopic undulations and thickness fluctuations in lipid bilayers from molecular dynamics simulations. *Biophys J* 79:426–433. doi:10.1016/S0006-3495(00)76304-1
 30. Almeida PFF, Vaz WLC (1995) In: Lipowsky R, Sackmann E (eds) *Handbook of biological physics*. Elsevier, New York, pp 305–357
 31. Seelig J (1977) Deuterium magnetic resonance: theory and application to lipid membranes. *Q Rev Biophys* 10:353–418
 32. Vermeer LS, De Groot BL, Réat V, Milon A, Czaplicki J (2007) Acyl chain order parameter profiles in phospholipid bilayers: computation from molecular dynamics simulations and comparison with 2H NMR experiments. *Eur Biophys J* 36:919–931. doi:10.1007/s00249-007-0192-9
 33. Petrasche HI, Dodd SW, Brown MF (2000) Area per lipid and Acyl length distributions in fluid Phosphatidylcholines determined by 2H NMR spectroscopy. *Biophys J* 79:3172–3192. doi:10.1016/S0006-3495(00)76551-9